Model for Human Use of Motion Cues in Vehicular Control

Ronald A. Hess*
University of California, Davis, Davis, California, 95616

A feedback model for human use of motion cues in tracking and regulation tasks is offered. The motion cue model is developed as a simple extension of a structural model of the human pilot, although other equivalent dynamic representations of the pilot could be used in place of the structural model. In the structural model, it is hypothesized that proprioceptive cues and an internal representation of the vehicle dynamics allow the human to create compensation characteristics that are appropriate for the dynamics of the particular vehicle being controlled. It is shown that an additional loop closure involving motion feedback can improve the pilot/vehicle dynamics by decreasing high-frequency phase lags in the effective open-loop system transfer function. Data from a roll-attitude tracking/regulation task conducted on a moving base simulator are used to verify the modeling approach.

Introduction

MANY manual control tasks such as automobile driving and aircraft piloting involve motion of the human operator. In addition to the visual and proprioceptive cues that are available to the human in such tasks, vestibular and kinesthetic cues are available from sensors in the inner ear and the skin and deep tissues. The manner in which such cues are utilized by the human operator in manual control tasks and the development of tractable models of the human operator in a motion environment have been the subject of considerable research (e.g., Refs. 1-3). A pertinent example of an activity in which such models can be of critical importance is the analytical assessment of manned flight simulator fidelity. Obviously, from an analytical standpoint, the study of simulation fidelity is dependent upon the existence of an accurate model of the human pilot in the flight and simulation environment, which obviously includes motion. The development and initial validation of such a model as a straightforward extension of an existing structural representation of the human pilot[4] is the subject of the research to be described.

For the purposes of the modeling effort of this study, the dynamics of the particular motion sensors, for example, the semicircular canals in the inner ear, will not be modeled. Rather, it will be assumed that linear acceleration or angular velocity cues are available to the human information processing system in the manual control task at hand. Modeling at an information processing level has been found to be an adequate approach for predicting the effects of motion cues on manual tracking/regulation performance[3] and is consistent with the level of physiological detail in the structural model of the human pilot that is to be used in this study.[4]

Structural Model with Motion Cues

Figure 1 is a block diagram of the structural model of the human pilot for a single-loop task. The model has been used in a variety of pilot vehicle studies, e.g., Refs. 4-7. The reader is referred to Ref. 8 for details. It is useful to at least summarize the manner in which the human is hypothesized to create compensation and utilize an internal model of the vehicle in tracking and regulation tasks. As evident in Fig. 1, the human is hypothesized to generate the compensation required in any task through proprioceptive feedback and not by any serial operation on the visual stimulus, $e(t)$. The general characteristics of this compensation (lead, lag, or simple attenuation) depend upon whether the proprioceptively sensed manipulator output $u_\delta(t)$ is integrated, differentiated, or simply attenuated in the frequency region around crossover. The required compensation is, in turn, dependent upon the vehicle dynamics in the region of crossover.[9] Finally, the crossover frequency is, itself, dependent upon task performance requirements and the target/disturbance bandwidth. The elements Y_f and Y_m in the structural model constitute the human's internal model of the vehicle in the crossover region.

Although the model of Fig. 1 is for a single-loop task, it can be applied to a multiloop task by considering successive loop closures around the "primary control loop," where the primary control loop is defined as that loop involving human interaction with a control manipulator. The structural model is employed only in this primary loop. For examples of multiloop application of the structural model, the reader is referred to Ref. 4.

Figure 2 shows the proposed modification of the structural model of Fig. 1 to include motion cues. Here, the rate of change of the primary control loop output variable $m(t)$ is simply fed back with gain K_v in parallel with the visual error $e(t)$, with gain K_e. A simplified form of Fig. 2 is shown in Fig. 3. Here, the m/u_1 transfer function of Fig. 2 has been approximated by the crossover model of the human:

$$G = [K \exp\{-\tau_e s\}]/s \tag{1}$$

One obvious caveat must be stated here, namely that the time rate of change of the output of the primary control loop must be capable of being sensed by the human vestibular system for the motion cue model to have face validity. Thus, for example, it would be inappropriate to employ this model in the vertical control loop of a hovering vehicle if the output of the primary control loop was vehicle vertical displacement, since vertical velocity could not be sensed by the vestibular system. However, a primary control loop output consisting of vertical velocity would be acceptable since vertical acceleration could be sensed by the vestibular system.

It is useful to quantify the performance improvements which would accompany the motion cue feedback shown in Figs. 2 and 3. Consider the error-to-target and error-to-disturbance transfer functions:

$$e/c = 1/\{1 + [GK_e/(1 + sGK_v)]\} \tag{2}$$

Received Aug. 1, 1988; revision received March 6, 1989.

*Professor, Division of Aeronautical Science and Engineering, Department of Mechanical Engineering. Associate Fellow AIAA.

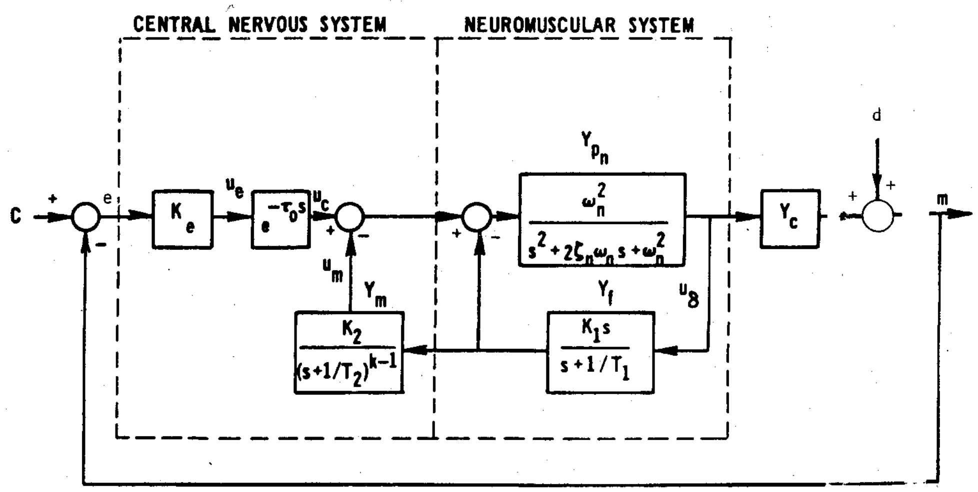

Fig. 1 Structural model of the human pilot.

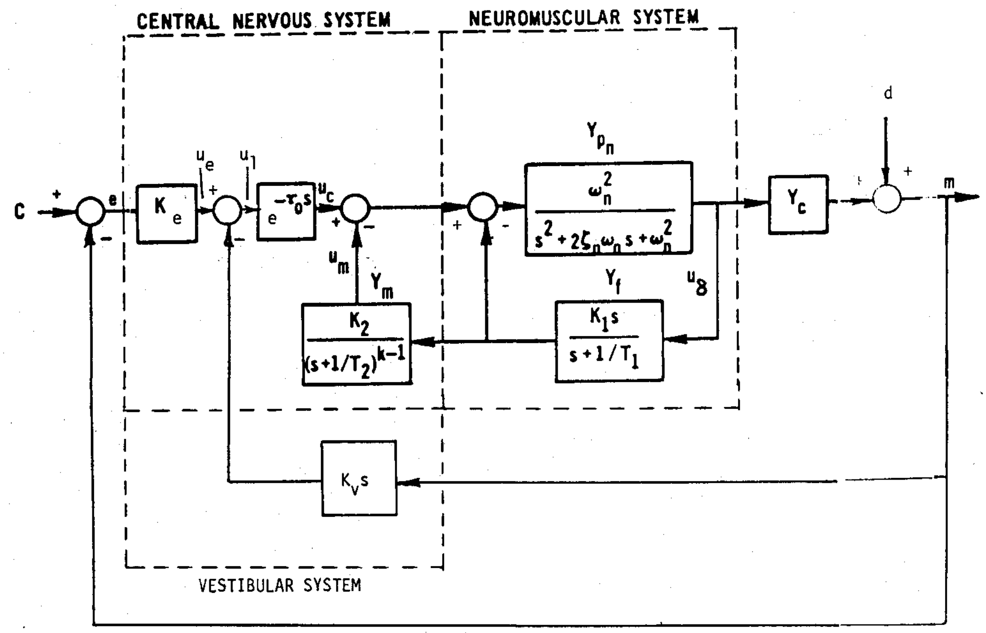

Fig. 2 Model for human use of motion cues.

and

$$e/d = -1/[1 + G(K_e + sK_v)] \quad (3)$$

Now, "effective" open-loop pilot/vehicle transfer functions can be defined for each of the previous closed-loop error transfer functions as

$$[G_c]_{\text{OL}} = GK_e/(1 + sGK_v) \quad (4)$$

$$[G_d]_{\text{OL}} = G(K_e + sK_v) \quad (5)$$

A first-order Padé approximation to the effective time delay τ_e can be employed to write G as

$$G = -[K(s - 2/\tau_e)]/[s(s + 2/\tau_e)] \quad (6)$$

By letting $a_1 = (1 + KK_v)$ and $a_2 = (1 - KK_v)$, $[G_c]_{\text{OL}}$ can be rewritten as

$$[G_c]_{\text{OL}} = -(KK_e/a_1)[(s\tau_e/2) - 1]/\{s[(s\tau_e a_2/2a_1) + 1]\} \quad (7)$$

Since $a_1 > a_2$, an examination of Eqs. (6) and (7) reveals that the effective open-loop target transfer function of Eq. (7) (motion feedback) will exhibit smaller high-frequency phase lags than those of GK_e (no motion feedback) and still retain the desirable integrator-like dynamics around crossover. In addition, a decrease in crossover frequency will result, but this can be compensated for by an increase in the gain K_e.

Similar results occur for $[G_d]_{OL}$. Here, Eq. (5) clearly shows that the motion cue feedback causes a zero to appear in the effective open-loop disturbance transfer function. With $K_v/K_e < 0.5$, Eq. (5) (motion feedback) will again exhibit smaller high-frequency phase lags than those of Eq. (1) (no motion feedback) and still retain the desirable integrator-like dynamics around crossover.

Again, employing Eq. (6), one can show that for closed-loop stability the motion feedback gain K_v must satisfy the following inequalities:

$$(K_e\tau_e/2) - (1/K) < K_v < 1/K \quad (8)$$

The motion cue feedback of Fig. 2 can thus be expected to lead to improved pilot/vehicle performance in both target tracking and disturbance regulation. What is most important is that these results will be valid regardless of the form of Y_c, since the motion loop was closed after the crossover model characteristics were obtained by the inner loops.

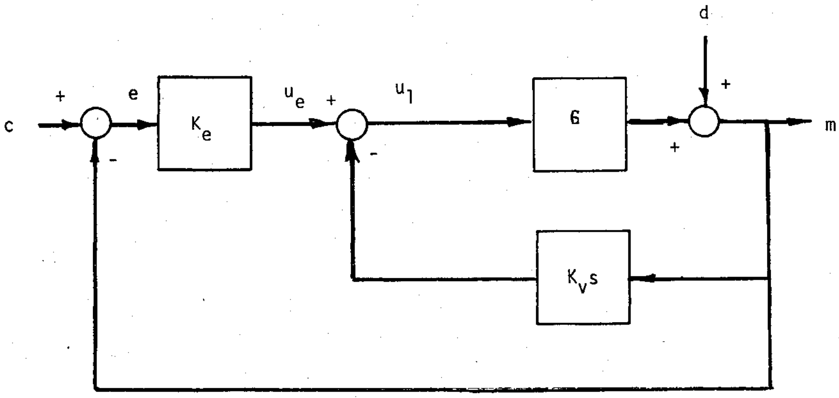

Fig. 3 Simplified version of Fig. 2.

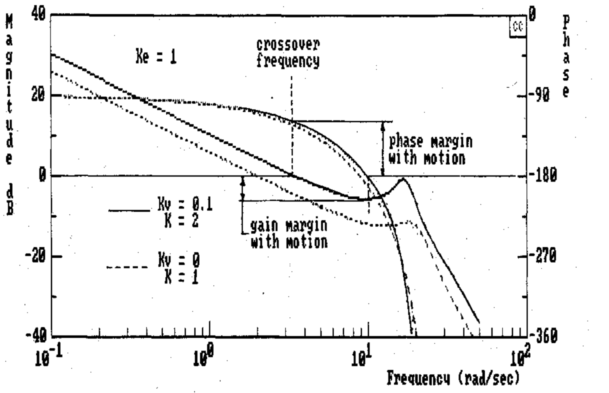

Fig. 4 Bode plot of effective target open-loop transfer function of system of Fig. 3.

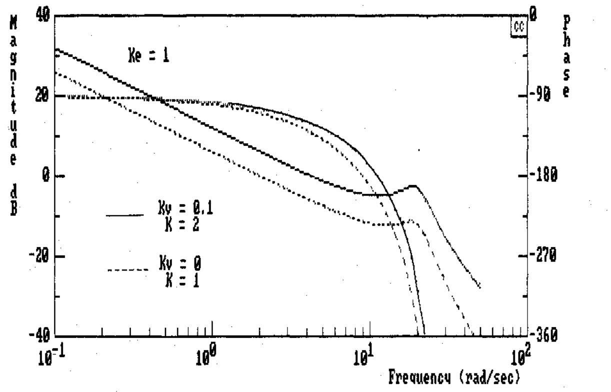

Fig. 5 Bode plot of effective disturbance open-loop transfer function of system of Fig. 3.

Figures 4 and 5 each show the Bode plots of the effective target and disturbance open-loop transfer functions [Eqs. (4) and (5)] with and without motion feedback ($K_v = 0.1$ and 0, respectively) in the case of a more realistic G, now given by

$$G = K(20)^2 \exp\{-0.1s\}/\{s[s^2 + 2(0.2)(20)s + (20)^2]\} \tag{9}$$

The quadratic term in the denominator of Eq. (9) approximates the closed-loop neuromuscular dynamics of the structural model of Figs. 1 and 2. The phase-lag differences caused by the motion feedback are interesting in that motion would appear to have the potential of improving performance in disturbance regulation to a greater extent than in target tracking since the phase lags in the effective open-loop transfer function are less in the former. Indeed, this result as been noted in simulation experiments.[3,10] By way of example, Fig. 6 shows the responses of the system of Fig. 3 to both step target and disturbance inputs, with and without motion feedback. For convenience, the disturbance step input has been chosen with an amplitude of -1, and the time delay in Eq. (9) has been represented by a fourth-order Padé approximation.

The preceding discussion was intended to demonstrate 1) how the structural model of the human pilot could be extended in a straightforward fashion to include motion cues in a manner independent of the form of the vehicle dynamics and 2) that significant performance improvements can accrue with the resulting motion feedback structure; that is, that there is some justification for the human pilot's adopting the motion feedback structure proposed in the model of Fig. 2. It is worth emphasizing that, at this juncture, as long as the crossover model is employed and the motion cues are fed back to the error signal as in Fig. 3, *any* pilot model could have been used in obtaining G. However, it was the structural model that suggested the motion feedback topology of Fig. 2, i.e., the hypothesis that proprioceIptive feedback forms the inner-most compensation loops in the pilot model leads to motion feedback being considered as an outer loop variable. The next section will present a comparison between the structural model and data from a well-documented manned flight simulation of a roll-attitude tracking/regulation task.

Roll-Attitude Tracking/Regulation Task

Figure 7 is a representation of the tracking/regulation task and cockpit display employed in the study of Ref. 10, a very thorough and well-documented study of roll-attitude tracking and regulation under motion and static conditions. Both target input and vehicle disturbances were used, and the motion simulator could be oriented so that the roll axis of the cab was either horizontal or vertical. In the latter case, the pilot was supine and the so-called "tilt cue," which the subjects could perceive when the roll axis was horizontal, was absent. The roll-attitude dynamics of the vehicle and simulator were given by

$$Y_c = 17(-s/25 + 1)/[s(s/1.6 + 1)$$
$$\times (s/5 + 1)(s^2/(11)^2 + 2(0.3)(11)s + 1)](\text{deg/s-lb}) \tag{10}$$

In the experiments of Ref. 10, the simulator dynamics consisting of the nonminimum phase zero and the quadratic pole were artificially included in the plant transfer function under static conditions. In addition to conducting the tracking/regulation tasks with cab-roll axis vertical or horizontal, a number of motion washout filters were evaluated in Ref. 10. One of these was selected for inclusion in the structural model validation herein and is given by

$$H_{wo} = s^2/[s^2 + 2(0.7)(0.85)s + (0.85)^2] \tag{11}$$

Figure 8 shows the structural model of Fig. 2 modified to include the tilt cue (K_tm) and the washout filter H_{wo}. The tilt cue

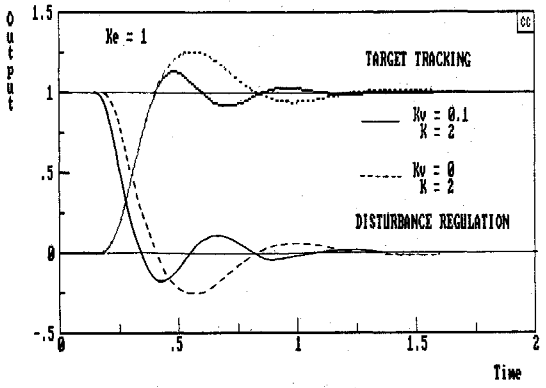

Fig. 6 Response of the system of Fig. 3 to a step target and disturbance inputs.

is simply attenuated primary control loop output, which, in this case, is roll attitude.

The effective open-loop target and disturbance transfer functions discussed in the previous section were measured in the experiments of Ref. 10. The target input and disturbance were implemented as sums of sinusoids. When the effective open-loop target transfer function for the static case obtained from the experiments of Ref. 10 was used, a trial and error procedure was employed to obtain a set of structural model parameters that resulted in the model transfer function of Eq. (4) closely matching the experimental transfer function. In Eq. (4), G is now the m/u_1 transfer function of Fig. 2. The selected model parameters are given in Table 1.

Now, *without changing the structural model parameters*, effective target open-loop transfer function comparisons between model and experiment were made as shown in Figs.

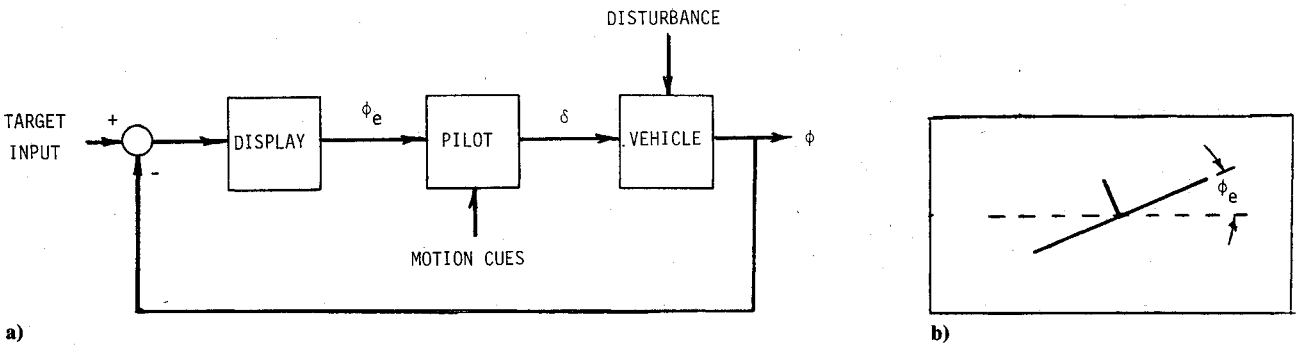

Fig. 7 The task and display of Ref. 10: a) roll-attitude tracking/regulation task and b) simulator display.

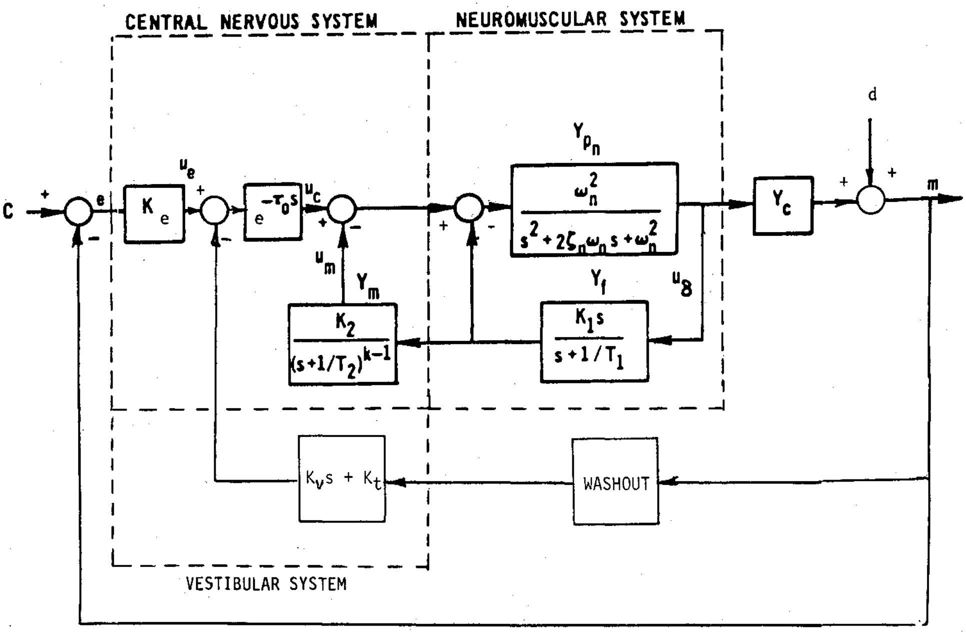

Fig. 8. Figure 2 modified to include tilt cue and motion washout.

Table 1 Parameter values for structural model

	Static	Tilt cue absent	Tilt cue present	Washout + tilt cue
K_e	1.0	1.0	1.0	1.0
K_1	1.25	1.25	1.25	1.25
K_2	10.0	10.0	10.0	10.0
T_1	100.0	100.0	100.0	100.0
T_2	0.625	0.625	0.625	0.625
ζ_n	0.75	0.75	0.75	0.75
ω_n	4.75	4.75	4.75	4.75
K_v	0.0	0.3	0.3	0.3
K_t	0.0	0.0	0.15	0.15
τ_0	0.1	0.1	0.1	0.1

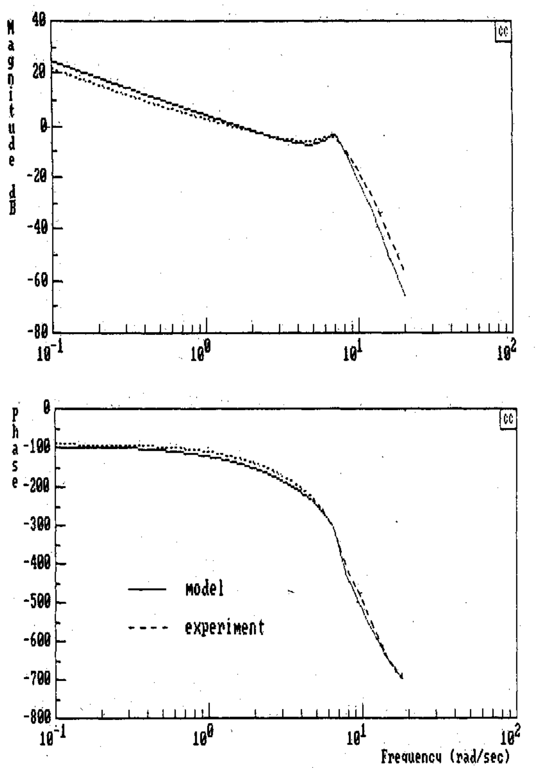

Fig. 9 Comparison of effective target open-loop transfer functions; experiment of Ref. 10 and motion cue model, static condition.

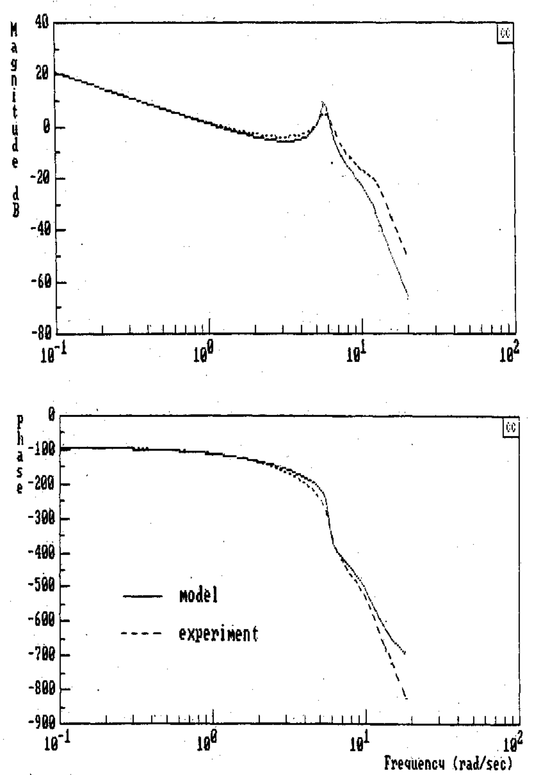

Fig. 10 Comparison of effective target open-loop transfer functions; experiment of Ref. 10 and motion cue model, motion with no tilt cue.

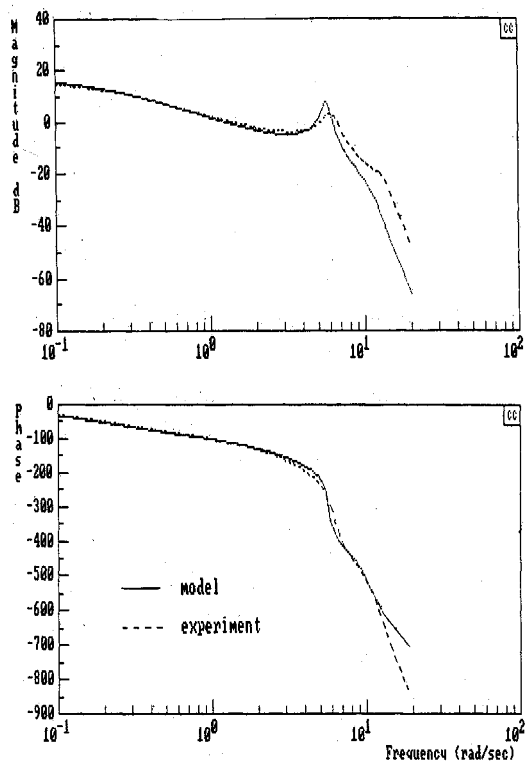

Fig. 11 Comparison of effective target open-loop transfer functions; experiment of Ref. 10 and motion cue model, motion with tilt cue.

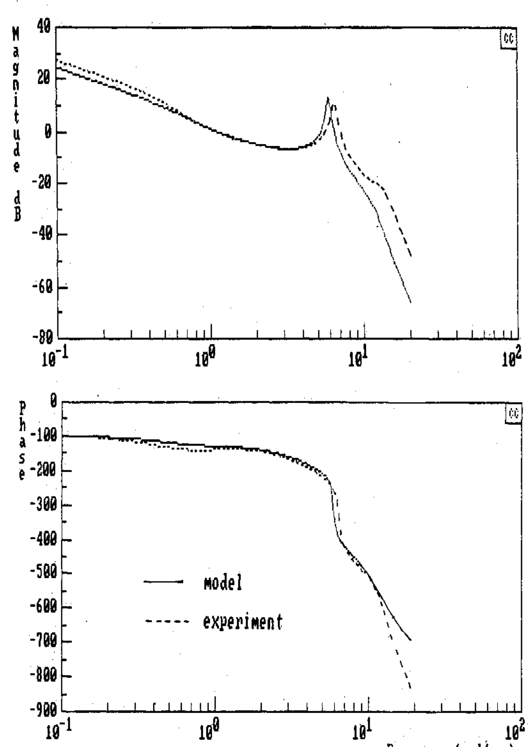

Fig. 12 Comparison of effective target open-loop transfer functions; experiment of Ref. 10 and motion cue model, motion with tilt cue and washout.

9–12. Here, only the magnitude of the gains K_v and K_t were selected to yield acceptable transfer function matches, and only one set of gain values were used. It should be noted that the curves denoted as "experiment" in these figures are actually the results of a 10-parameter model fit through the discrete amplitude and phase values obtained from fast Fourier transforms (FFT) at the seven target input frequencies. These model fits were used in lieu of the FFT results since the latter were not reported for all of the test configurations, whereas the model parameters were. The discrepancies appearing in the higher frequency amplitudes in Figs. 9–12 are of little concern since the phase comparisons are quite acceptable and only two target frequencies (6.98 and 11.85 rad/s) determined the shape of the amplitude curves above 4.1 rad/s.

As just mentioned, and as Table 1 indicates, no changes in the structural model parameters were made in matching the experimental results for the various motion conditions. The appropriate motion feedback gains (K_v and K_t) and the washout filter were either included or excluded. This, in itself, is an important result. In terms of the structural model, it suggests that the human *does not alter* the characteristics of his inner proprioceptive feedback loops in the presence or absence of motion; rather, these characteristics are dictated by the vehicle dynamics in the primary control loop and the task demands.

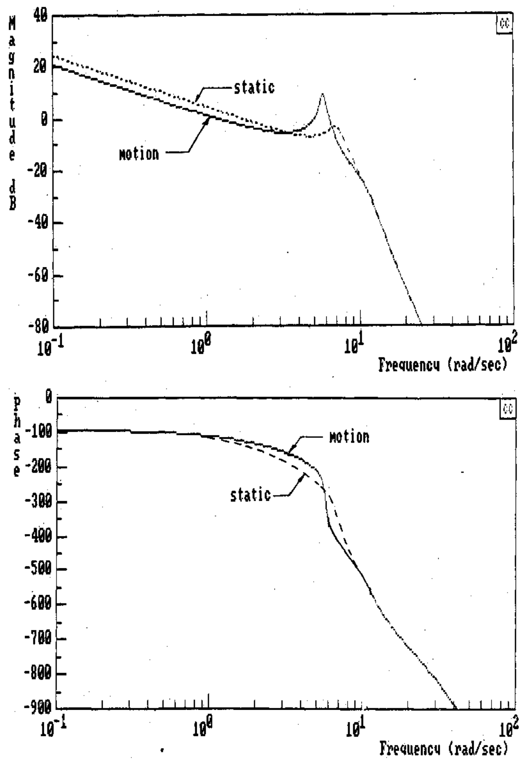

Fig. 13 Comparison of effective target open-loop transfer functions; motion cue model, static and motion (no tilt cue).

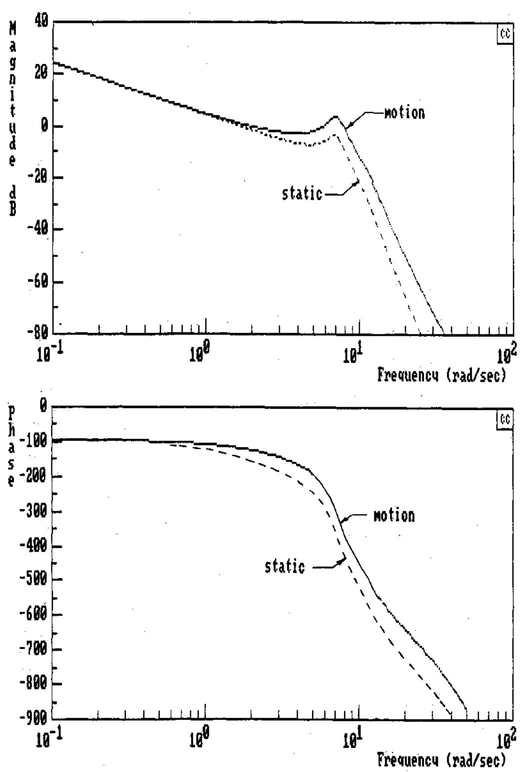

Fig. 14 Comparison of effective disturbance open-loop transfer functions; motion cue model, static and motion (no tilt cue).

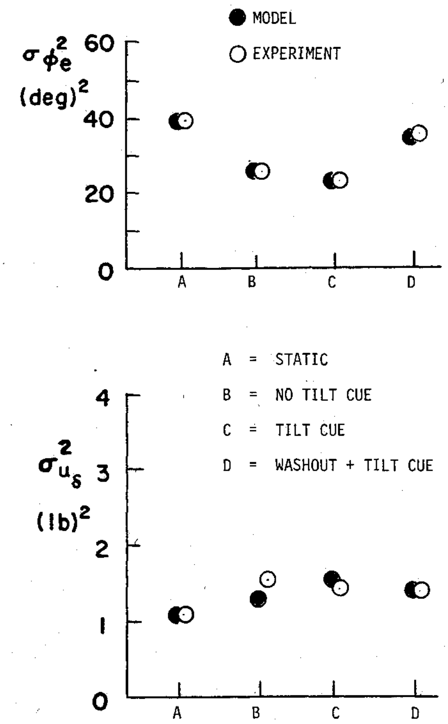

Fig. 15 Comparison of error and control scores; experiment of Ref. 10 and motion cue model.

Figures 13 and 14 compare the effective open-loop target and disturbance transfer functions for the motion cue model. The comparisons are quite similar to those in Figs. 4 and 5 if the same K values were used in these earlier figures. As in Figs. 4 and 5, the largest phase improvement occurs with the disturbance transfer function.

Figure 15 is a comparison of the error and control scores reported in Ref. 10 for simultaneous target tracking and disturbance regulation with the scores generated by the structural model in a digital simulation of the roll tracking/regulation tasks. The experimental conditions correspond to those of Figs. 9–12. The digital simulation employing the structural model did not include remnant injection. However, since the performance data of Ref. 10 clearly indicates the part of the error and control scores attributable to operator remnant, a direct comparison between model and simulation results was still possible. The performance comparisons of Fig. 15 are quite good, which is not unexpected, given the quality of the transfer function matches of Figs. 9–12. It should be noted that the presence of motion cues leads to a 35% reduction in the mean square tracking error for both model and experiment (comparing cases A and B in Fig. 15).

The preceding discussion was intended to validate the motion cue model of Fig. 2 by demonstrating that the model could match pilot/vehicle transfer functions and performance scores obtained from a well-documented simulation study in which the nature of vehicle motion was carefully and systematically varied. The fact that acceptable matches could be obtained with no variation in inner-loop structural model parameters is particularly noteworthy. Once again, any pilot model that would lead to the pilot/vehicle characteristics shown in Fig. 10 (no motion) could be employed in the motion cue model discussed herein.

Discussion

The motion cue model of Fig. 2 and the results of the previous section are not without theoretical implications as regards human use of motion cues in vehicular control. In terms of the model, human fundamental compensation for the vehicle dynamics in the primary control loop are not created by motion feedback. Motion feedback merely serves to "tune" the pilot/vehicle dynamics to improve tracking performance by decreasing the high-frequency phase lags occurring in the effective open-loop pilot/vehicle transfer functions *after* the fundamental pilot compensation occurs.

It should be noted that the motion cue model developed herein using the structural model is completely compatible with the handling qualities theory developed in Ref. 4 and the preview control model for the human pilot developed in Ref. 11.

Conclusions

Based on the analyses discussed herein, the following conclusions can be drawn:

1) A model for human use of motion cues in vehicular control can be obtained by a simple extension of existing representations of human pilot behavior in static tracking.

2) The motion cue model involves only the feedback of attenuated vehicle output rate in the primary control loop in a vehicle control task, i.e., higher derivatives of the output are not required.

3) In terms of the model, motion feedback does not provide fundamental compensation in the tracking or regulation task.

4) The motion cue model implemented as an extension of the structural model was able to match experimental results from manned simulation with different motion conditions without the necessity of changes in model parameters that are appropriate for tracking in static conditions.

Acknowledgment

This research was supported by Grant NAG 2-482 from the U.S. Army Aeroflightdynamics Directorate at NASA Ames Research Center, Moffett Field, California. Adolph Atencio Jr. was the contract monitor.

References

[1]Stapleford, R. L., Peters, R. A., and Alex, F., "Experiments and a Model for Pilot Dynamics with Visual and Motion Inputs," NASA CR-1325, May 1969.

[2]Curry, R. E., Hoffman, W. C., and Young, L. R., "Pilot Modeling for Manned Simulation." Air Force Flight Dynamics Lab., Wright Patterson AFB, OH, AFFDL-TR-76-124, Dec. 1976.

[3]Levison, W. H., and Junker, A. M., "A Model for the Pilot's Use of Motion Cues in Roll-Axis Tracking Tasks," Air Force Aerospace Medical Research Laboratory, Wright-Patterson AFB, OH, AMRL-TR-77-40, June 1977.

[4]Hess, R. A., "A Theory for Aircraft Handling Qualities Based Upon a Structural Pilot Model," *Journal of Guidance, Control, and Dynamics* (to be published).

[5]Hess, R. A., "A Rationale for Human Operator Pulsive Control Behavior," *Journal of Guidance and Control*, Vol. 12, No. 6, 1989, pp. 792–797.

[6]Hess, R. A., "Pursuit Tracking and Higher Levels of Skill Development in the Human Pilot," *IEEE Transactions on Systems, Man, and Cybernetics*, Vol. SMC-11, No. 4, 1981, pp. 262–273.

[7]Hess, R. A., "A Model-Based Investigation of Manipulator Characteristics and Pilot/Vehicle Performance," *Journal of Guidance, Control, and Dynamics*, Vol. 6, No. 5, 1983, pp. 348–354.

[8]Hess, R. A., "A Model-Based Theory for Analyzing Human Control Behavior," *Advances in Man-Machine Systems Research*, Vol. 2, edited by W. B. Rouse, JAI Press, Greenwich, CT, 1985, pp. 129–175.

[9]McRuer, D. T., and Krendel, E., "Mathematical Models of Human Pilot Behavior," AGARDograph 188, 1974.

[10]Jex, H. R., Magdaleno, R. E., and Junker, A. M., "Roll Tracking Effects of *G*-Vector Tilt and Various Types of Motion Washout," *Proceedings of the Fourteenth Annual Conference on Manual Control*, NASA CP2000, April 1978, pp. 463–502.

[11]Hess, R. A., and Chan, K. K., "Preview Control Pilot Model for Near-Earth Maneuvering Helicopter Flight," *Journal of Guidance, Control, and Dynamics*, Vol. 11, No. 2, 1988, pp. 146–152.